International Journal of Pharmacology

Int. J. Pharmacol. **2025**; 21(8): 45965
https://doi.org/10.31083/IJP45965

Research Article

Colon Cancer Cells Exhibited Multi-Phase Death Networks After Sustained Exposure to the Carrageenan–Soy Protein Mixture

Alawiah Alhebshi[1,*], Safiyah Alzahrani[1,2]

[1]Department of Biological Sciences, Faculty of Science, King Abdulaziz University, 21589 Jeddah, Saudi Arabia
[2]Department of Basic Medical Sciences, College of Applied Medical Sciences, King Khalid University, 61421 Khamis Mushait, Saudi Arabia
*Correspondence: aalhebshi@kau.edu.sa (Alawiah Alhebshi)

Academic Editor: Mehmet Ozaslan
Submitted: 21 August 2025 Revised: 27 September 2025 Accepted: 10 October 2025 Published: 16 December 2025

Abstract

Background and Objectives: This investigation was driven by the growing interest in natural cancer therapeutics, which aim to minimize the side effects of chemical treatments and enhance immunity. Thus, this study aimed to assess the impacts of a carrageenan/soy protein mixture on Human Colorectal Tumor Cells (HCT-116) colon cancer cells through pathway regulation and cell death assessment. **Methods**: This experiment compared the treated HCT (THCT) cells exposed to a carrageenan/soy protein mixture (0.25/0.05 mg/mL) with the untreated control cells (UNT) over the experimental durations of 24, 48, and 72 hours. **Results**: The treatment triggered sophisticated cell death dynamics, characterized by progressive morphological changes. Viability displayed a fascinating pattern—decreasing to 78.8% at 24 h ($p < 0.001$) before partially recovering to 86.86% by 72 h ($p = 0.018$). Death mechanisms showed remarkable temporal organization: early apoptosis appeared exclusively at HCT 24 h ($p = 0.0056$), late apoptosis peaked early then declined, while necrosis followed a wavelike progression: initially high, dropping at 48 h ($p = 0.0183$), then dramatically surging by 72 h ($p < 0.0001$) to become the dominant death mode. Gene expression correlations analysis underwent striking temporal reconfiguration: 24 h showed *BAX* expression correlating with *Bcl-2* and *NF-kB* ($p < 0.01$) and a strong association with *Notch-1*/2 ($p < 0.0001$); by 48 h, the correlations for *BAX* had weakened while *NF-kB* formed negative relationships with *Bcl-2* ($p < 0.001$) and positive ones with *Notch-1* and *HSE-1* ($p < 0.001$); at 72 h, *Bcl-2*/*Notch-1* aligned powerfully ($p < 0.001$) while *HSE-1* developed significant negative correlations with most genes, particularly *Notch-2* ($p < 0.0001$) and *NF-kB* ($p < 0.001$). **Conclusion**: The natural carrageenan–soy mixture triggered a three-stage death process in colon cancer cells, with a surprising 72-hour phase where cells looked healthier but were dying. This pattern altered key gene activity, disrupting the cancer cell survival process and offering a promising new approach to target the metabolism of stubborn cancers.

Keywords: HCT-116 colon cancer cells; carrageenan; soy protein; natural therapeutics; apoptosis; necrosis; cell viability; *NF-kB*; notch signaling; gene expression regulation

1. Introduction

Cancers (in particular colorectal cancer) are a significant worldwide health problem, developing through progressive genetic and epigenetic changes [1]. The disease pathway involves both the inactivation of tumor suppressors and the activation of oncogenes [2]. However, chemotherapy remains a standard treatment approach; it frequently causes undesirable side effects, and treatment resistance can be generated [3]. The body's natural defense against CRC involves the coordinated action of multiple gene families. Apoptotic regulators such as p53 and *BAX* function to eliminate potentially cancerous cells, though p53 mutations occur in approximately 75% of colorectal malignancies [4]. Inflammatory mechanisms exhibit context-dependent effects, initially protecting acute inflammatory responses but potentially becoming carcinogenic when chronically activated via the COX-2 and TNF-α pathways [5]. Growth regulation depends on cell survival genes, including AKT and mTOR signals, that normally prevent aberrant cell proliferation [6]. Genomic integrity relies on DNA repair genes, whose impairment characterizes roughly 15% of colorectal cancers [7]. Together, these genetic systems constitute a multilayered protective network that, when functioning optimally, prevents colorectal carcinogenesis through coordinated cell death, inflammatory modulation, and growth control [8].

Avoiding the weaknesses of traditional cancer therapies (toxic side effects and treatment resistance) [9]. Previous study are now exploring nature's products for better solutions [10]. Two compounds have captured significant attention: carrageenan (extracted from red seaweed) [11] and soy protein [12]. This natural pair showed remarkable promise in fighting cancer in general, colorectal cancers in particular, offering a gentler yet potentially powerful approach to targeting these challenging malignancies [13].

Carrageenan offers substantial promise as an anticancer agent due to its multifaceted mechanisms of action and natural origin [11]. It can induce apoptosis in human colorectal cancer cells through activation of caspase-dependent pathways [14]. Carrageenan compound exhibits

directed cytotoxicity toward malignant cells while sparing normal tissues, resulting in significant growth inhibition in breast cancer cell lines with minimal effect on healthy mammary epithelial cells [15]. Carrageenan downregulates Vascular Endothelial Growth Factor (VEGF) expression and has the capability of suppressing angiogenesis, thereby limiting tumor vascularization [16]. Additionally, it enhances immunomodulatory properties by stimulating natural killer cell activity and promoting anti-tumor immune responses [17]. Furthermore, it can overcome multidrug resistance mechanisms in cancer cells, potentially addressing significant limitations of conventional chemotherapies [18], as well as reducing tumor burden in animal models of colorectal cancer [19].

Soy protein demonstrates remarkable anticancer potential through multiple well-documented mechanisms. The abundant isoflavones found in soy [20], especially genistein and daidzein, demonstrate significant capacity to inhibit cancer growth that relies on hormonal pathways for development and progression [21]. Isoflavone is a selective estrogen receptor modulator, resulting in substantial growth inhibition in breast cancer cells through estrogen receptor antagonism [22], and it can induce apoptosis via intrinsic pathways in prostate cancer models [23]. Additionally, it acts similarly to carrageenan, where it has the same capacity to limit tumor vascularization that inhibits angiogenesis through downregulation of VEGF signaling [24]. The anti-inflammatory properties of soy protein peptides [25] confirmed the suppression of *NF-kB* activation, reducing tumor-promoting inflammation [26]. Moreover, specific bioactive peptides found in soy protein can block essential enzymes involved in cancer progression, such as matrix metalloproteinase [27].

Otherwise, carrageenan's anticancer limitations include poor bioavailability [28], potential proinflammatory effects in intestinal tissue [29], inconsistent efficacy across different cancer types [11], difficulties in standardization due to batch variability [30], and poorly characterized drug interactions [11]. These factors restrict its practical therapeutic potential despite promising laboratory results [28]. Soy protein's anticancer efficacy faces critical constraints: inconsistent isoflavone concentrations (50–300 mg/100 g) from agricultural and processing variables [12]; concerning estrogenic activity that may promote certain hormone-responsive tumors [31]; limited bioavailability, with most genistein lost before reaching target tissues [21]; unpredictable metabolism due to gut microbiome diversity [32]; and reduced bioactive compound accessibility through food matrix effects [33].

Given the limitations of both compounds and the urgent need for effective natural treatments for colorectal cancer, this study explored the impact of combining carrageenan and soy protein on critical regulatory pathways in HCT-116 colon cancer cells at various time points. This current research focused on tracking changes in the regulations of gene expression related to apoptosis, inflammation, and cell survival, while also measuring the rate of apoptosis in these cancer cells after treatment with the combination. This approach aimed to uncover the potential of a carrageenan-soy protein blend as a promising strategy for targeting colorectal cancer.

2. Materials and Methods

2.1 Cell Culture and Treatment of HCT-116 Colon Cancer Cell Line

HCT-116 colon cancer cells (ATCCCCL247™) were maintained in DMEM supplemented with 10% FBS at 37 °C, with viability monitored using Trypan blue and passaging performed at 70% confluence. The cell line was validated by STR profiling and tested negative for mycoplasma. The study compared untreated control cells (UNT) with the THCT group that received a combination of κ-Carrageenan (Signa Aldrish part of the Merck KGaA, Darmstadt, Germany group, Cat No. 11114-20-8) and soy protein (Product code: NCS-57380, iHerp, Irvine, CA, USA) (THCT), which were sterilized by filtration and administered at 0.25/0.05 mg/mL, respectively, per 5000 cells. Both treated and untreated HCT cell groups were harvested at specific intervals (24-, 48-, and 72-hours post-treatment) to enable thorough temporal analysis of cellular responses [13].

2.2 Assessment of HCT Colon Cancer Cell Survival and Programmed Cell Death Following Experimental Intervention

We assessed cellular responses using two complementary methods. For viability testing, HCT-116 cells were cultured in 96-well plates (5×10^3 cells/well) for 24 hours before receiving either no treatment (UNH) or the carrageenan/soy protein formulation (THCT). The MTT metabolic assay was then performed by adding MTT solution to fresh media, allowing 4 hours for formazan crystal formation, and dissolving these crystals with DMSO before spectrophotometric measurement at 540 nm.

To evaluate apoptotic effects, we seeded cells more densely (2×10^6 cells/flask) and exposed them to brief 5-minute treatments followed by extended incubation periods (24–72 hours). These cells were then processed for flow cytometric analysis using the FITC Annexin V/V/propidium iodide dual staining method, which distinguishes between early apoptotic, late apoptotic, and necrotic cell populations with high sensitivity.

2.3 Transcriptional Profile Characterization in HCT Colorectal Carcinoma Cells Following Therapeutic Exposure

HCT-116 cells were densely cultured (6×10^6 cells per flask) and subjected to experimental treatments before being collected at predetermined time points. Total RNA was isolated using the high-yield QIAGEN RNeasy® Midi

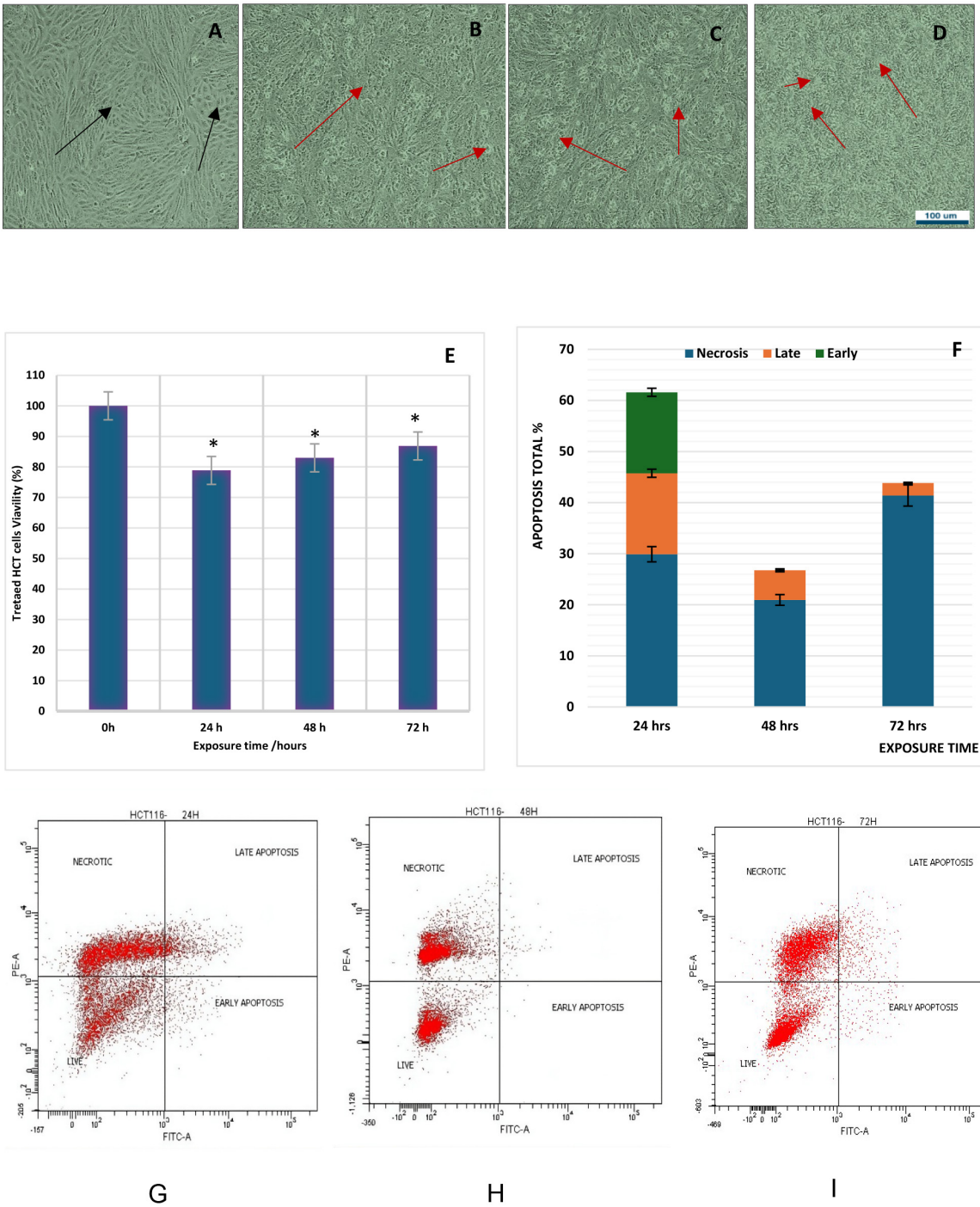

Fig. 1. Temporal progression of cell death in HCT colorectal cancer cells exposed to carrageenan-soy protein mixture. (A) Morphological appearance of untreated control cells, with black arrows indicating normal cellular features. (B) Morphological alterations observed in treated cells after 24 h, with red arrows showing apoptotic characteristics. (C) Morphological changes in treated cells after 48 h, with red arrows indicating apoptotic features. (D) Morphological changes in treated cells after 72 h, with red arrows highlighting apoptotic characteristics. Images were captured at 400× magnification. (E) Cell viability was measured over time from 0 to 72 hours, demonstrating statistically significant differences ($p < 0.05$) across four independent experiments. In the figure, asterisks (*) denote significant differences between the untreated control cells (UNT) and the treatment group at the respective time points. (F) Quantitative analysis of cell death pathways demonstrating the treatment's impact on apoptosis stages, with statistically significant outcomes ($p < 0.05$) from four independent experiments. (G–I) Flow cytometry plots illustrating the distribution of cell populations at 24 h, 48 h, and 72 h, respectively, differentiating viable, early apoptotic, late apoptotic, and necrotic cells. Scale bar = 100 µm.

Table 1. Sequence details of gene-specific primers used for quantitative real-time PCR analysis of apoptotic and signaling pathway markers.

Primer name	Position	Primer sequence	Primer length
BAX	sense	CCTGTGCACCAAGGTGCCGGAACT	24
	antisense	CCACCCTGGTCTTGGATCCAGCCC	24
BCL-2	sense	TTGTGGCCTTCTTTGAGTTCGGTG	24
	antisense	GGTGCCGGTTCAGGTACTCAGTCA	24
CXCR-4	sense	TTCTACCCCAATGACTTGTG	20
	antisense	ATGTAGTAAGGCAGCCAACA	20
GAPDH	sense	GCACCGTCAAGGCTGAGAAC	20
	antisense	TGGTGAAGACGCCAGTGGA	19
HSE-1	sense	CCAGTTTGCTTTCCTCATTCC	21
	antisense	TCTTCTCTCCCAGTATTCAAGTTCC	25
Jadded-1	sense	AGCGACCTGTGTGGATGAG	19
	antisense	GGCTGGAGACTGGAAGACC	19
NF-kB	sense	ATCCCATCTTTGACAATCGTG C	22
	antisense	CTGGTCCCGTGAAATACACCTC	22
Notch-1	sense	GACATCACGGATCATATGGA	20
	antisense	CTCGCATTGACCATTCAAAC	20
Notch-2	sense	TGACAACAGCAACAGCAAGG	20
	antisense	GATGCCACCTGAACAACTGC	20

Kit protocol (Cat. No. 74134, QIAGEN, Manchester, UK), followed by reverse transcription to cDNA using Promega's ImProm-II™ system. Transcriptional changes were measured using quantitative real-time PCR, which combined the high-sensitivity BioFact™ Master Mix (Cat. No. DQ362-40h, BIOFACT Co., Ltd., Daejeon, Korea) with precisely designed oligonucleotide primers targeting key regulatory genes (sequences provided in Table 1), enabling accurate amplification and detection of even subtle expression differences between treatment conditions. Gene expression data were calibrated against the consistently expressed reference gene GAPDH, serving as an internal control. The widely validated $2^{-\Delta\Delta Ct}$ algorithm was then applied to quantify relative transcriptional changes.

2.4 Statistical Methods and Visual Data Representation.

We performed statistical evaluation using MegaStat software (version 10.2.2.1, J.B. Orris, Butler University, Indianapolis, IN, USA) to determine treatment efficacy. The analytical approach employed one-way ANOVA to examine both internal control group variability and the differential responses between experimental and control cells, with results considered statistically significant at $p < 0.05$. We studied how target genes relate to each other using a simple Python system. We used NumPy for calculations, pandas to organize our data, and seaborn to make clear visual charts.

3. Results

3.1 Carrageenan-Soy Protein Treatment Induces Apoptotic Features in HCT-116 Cells

The morphological reconfiguration of HCT adenocarcinoma epithelium exhibited pronounced progression throughout the 72-hour carrageenan-soy protein treatment protocol. Untreated control HCT exhibited prototypical epithelial cytomorphology—displaying uniformly spheroid to ellipsoid cellular conformations with distinctly demarcated central nuclei and well-defined microvillous projections emanating from their intact plasma membranes (Fig. 1A). The 24-hour timepoint analysis revealed initial cytological transformation, with discrete cellular subsets demonstrating unequivocal early-phase apoptotic phenomena: quantifiable cytoplasmic retraction, nascent plasmalemmal evaginations, and preliminary disruption of cellular ultrastructure (Fig. 1B). At 48 hours post-treatment, this apoptotic phenotype had amplified substantially across the specimen field, characterized by accentuated cytosolic compaction, elaborate membrane vesiculation, comprehensive cytoskeletal disorganization, and significant nucleo-morphological alterations, including chromatin condensation and karyorrhexis throughout the experimental population (Fig. 1C). The 72-hour assessment revealed a noteworthy homeostatic plateau, where cellular samples maintained their established apoptotic ultrastructure without further morphological progression beyond the cytological state established during the preceding temporal interval (Fig. 1D).

Quantitative viability assessments revealed a biphasic cellular response to HCT cells treated with carrageenan-soy protein treatment. At all examined time points—24, 48, and 72 hours—HCT cells exposed to the soy protein–carrageenan mixture displayed a significant reduction in viability compared with the untreated control group, with p values recorded at <0.05 for each interval. The compound initially exerted potent cytotoxicity, reducing viable cell populations to 78.8% at 24 hours post-exposure

to the carrageenan/soy protein treatment compared to the untreated control cells (UNT) ($p < 0.001$). A gradual increase followed this acute toxic phase, with carrageenan and soy protein-cell viability increasing to 82.95% by 48 hours, while maintaining significant differences from the untreated control populations ($p = 0.03$). The recovery trajectory continued through 72 hours, with viability further improving to 86.86%, although still statistically lower than that of untreated cells ($p = 0.018$). During the current observation period, cell viability showed a consistent reduction at the 24-hour mark and continued to rise throughout the 72-hour timeframe. However, the differences in viability between these sequential time intervals did not reach statistical significance (Fig. 1E).

Treatment with carrageenan/soy protein triggered a distinct death pattern in HCT cells over time. Necrosis dominated the response, following a wavelike trajectory—high at 24 hours, dipping at 48 hours ($p = 0.0183$ versus 24 h), then surging dramatically by 72 hours to levels significantly higher than both earlier timepoints ($p = 0.0043$ versus 24 h; $p = 0.0000$ versus 48 h). Meanwhile, early apoptosis exhibited a distinct profile, becoming significant only at 24 hours ($p = 0.0056$) before disappearing entirely at later timepoints. This brief apoptotic response accounted for approximately 18% of total cell death, occurring exclusively during the first day, creating a stark contrast with the sustained and ultimately intensifying necrotic cell death observed throughout the experiment. Late apoptosis displayed a distinctive temporal signature, peaking significantly at 24 hours compared to all other timepoints (48 and 72 hours), then declining at 48 hours and stabilizing at 72 hours. Late apoptosis accounted for approximately 25% of the cumulative cell death response, with the 24 hours again providing the most considerable contribution (Fig. 1F–I).

3.2 Expression of Apoptotic Markers in HCT Cells Following the Carrageenan/Soy Protein Treatment

HCT cells treated with carrageenan/soy protein mixture induced a significant *BAX* gene upregulation across all time points. Expression followed a distinct pattern: consid-

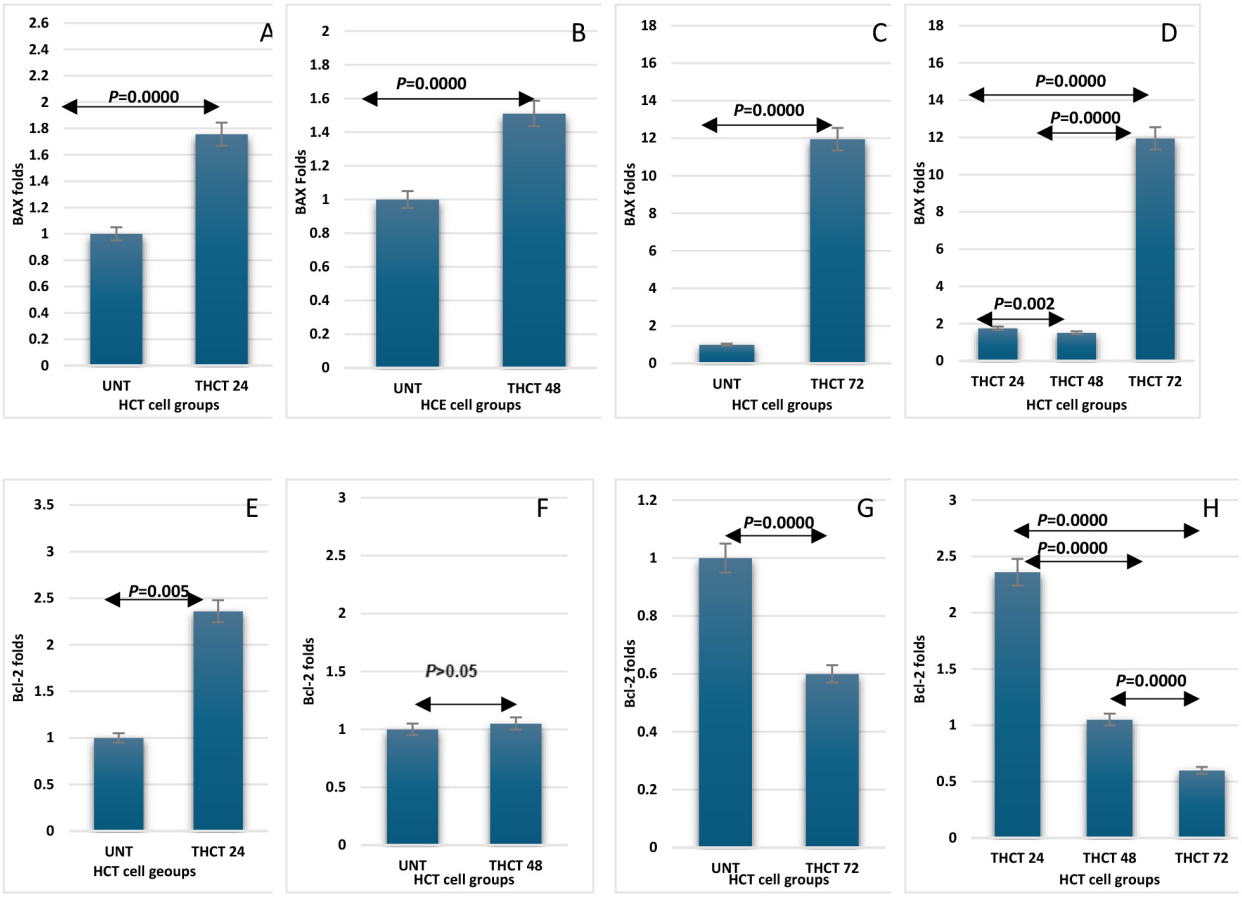

Fig. 2. Time-course analysis of BAX and BCL-2 mRNA levels in HCT cells following treatment with the carrageenan/soy protein formulation. UNT denotes untreated control cells, and THCT refers to cells treated with the carrageenan/soy protein mixture. Statistical differences between groups were evaluated using one-way ANOVA ($p < 0.05$). (A) BAX expression at 24 hours; (B) at 48 hours; (C) at 72 hours. (D) BAX expression compared across all time points. (E) BCL-2 expression at 24 hours; (F) at 48 hours; (G) at 72 hours; and (H) comparative BCL-2 expression at all time points.

erable elevation at 24 hours compared to untreated controls ($p < 0.001$) (Fig. 2A), continued elevation but at lower levels at 48 hours ($p < 0.001$) (Fig. 2B), and peak expression at 72 hours (Fig. 2C). The 72-hour timepoint displayed the most robust *BAX* levels, significantly exceeding both baseline and earlier measurements ($p < 0.001$ for both comparisons) (Fig. 2D).

BCL-2 gene expression exhibited a complex profile in HCT cells after exposure to a carrageenan and soy protein mixture. Treatment triggered significant *BCL-2* upregulation at 24 hours compared to the untreated controls ($p = 0.005$) (Fig. 2E), followed by a return to baseline levels at 48 hours, with no statistical difference from the untreated controls (Fig. 2F). *BCL-2* gene expression exhibited a second significant increase at the 72-hour time point compared to untreated control baseline levels ($p < 0.001$) (Fig. 2G). The highest expression of *BCL-2* levels was observed at 24 hours, significantly exceeding those at later time points ($p < 0.001$). The 72-hour measurements showed a marked decline from 48-hour levels ($p < 0.001$), reaching the lowest *BCL-2* expression observed during the experiment (Fig. 2H).

3.3 Temporal Regulation of NF-kB Expression After Carrageenan/Soy Protein Treatment

The present *NF-kB* expression levels exhibited a precise time-dependent expression profile after carrageenan/soy protein administration to the HCT cells. The current treatment initiated a significant inflammatory response, marked by substantial *NF-kB* upregulation at 24 hours compared to untreated controls ($p = 0.0001$) (Fig. 3A). This elevated expression in the current treated group persisted for 48 hours, remaining significantly higher compared to the untreated control level ($p < 0.0001$) (Fig. 3B). By 72 hours, *NF-kB* expression decreased below control values. However, this difference lacked statistical significance (Fig. 3C).

Analysis of the expression revealed maximum *NF-kB* levels at 24 hours, which were significantly higher than those measured at both 48 hours ($p = 0.0018$) and 72 hours ($p = 0.001$). The 48-hour timepoint showed slight upregulation of expression, lower than the initial peak but still significantly elevated compared to 72-hour levels ($p < 0.001$). This expression pattern demonstrates a systematic attenuation of the inflammatory signal over the three-day experimental course (Fig. 3D).

3.4 Temporal Regulation of Cell Signaling Expression After Carrageenan/Soy Protein Treatment

Notch-1 exhibited a distinctive biphasic expression pattern in response to carrageenan/soy protein treatment. The carrageenan/soy protein formulation generated a biphasic *Notch-1* expression pattern, with significant upregulation at both 24 and 72 hours compared to untreated controls ($p = 0.0000$ and 0.0032, respectively) (Fig. 4A,C). However, the expression pattern of this target gene showed a distinct interruption at 48 hours, when *Notch-1* levels reversed course and dropped below control values, though this decrease did not reach statistical significance (Fig. 4B). Temporal comparison within the treatment group demonstrated that *Notch-1* mRNA expression reached its maximum at 24 hours, significantly overwhelm the levels observed at both 48 and 72 hours ($p < 0.001$ for both comparisons), while the 48-hour measurement represented the lowest point of *Notch-1* expression throughout the experimental period, showing significant reduction compared to the subsequent 72-hour expression levels ($p < 0.001$) (Fig. 4D).

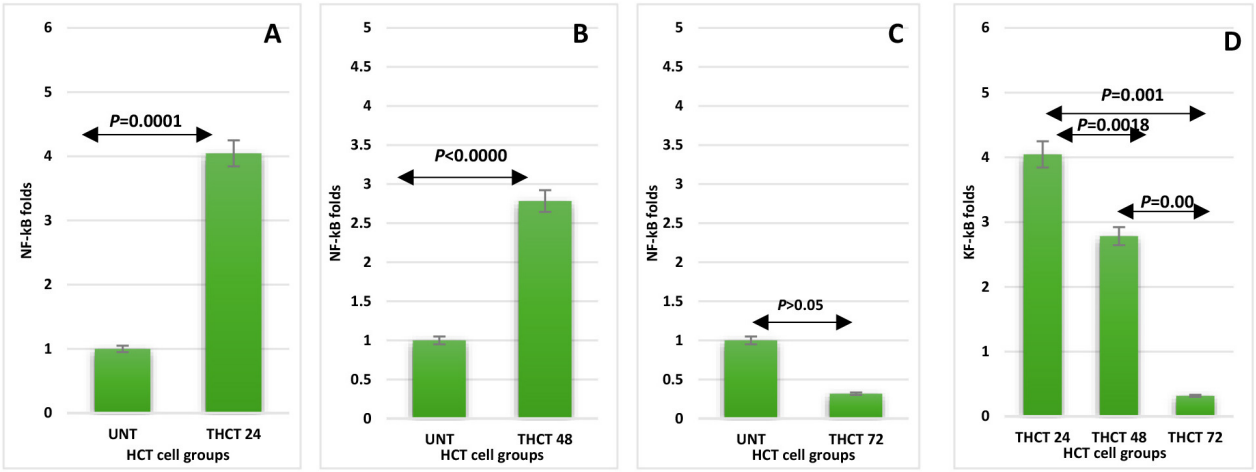

Fig. 3. Time-course analysis of *NF-kB* regulatory gene levels in HCT cells treated with carrageenan/soy protein formulation. UNT denotes untreated control cells, and THCT refers to cells exposed to the carrageenan/soy protein formulation. Panels show NF-*k*B expression at (A) 24 h, (B) 48 h, and (C) 72 h, with (D) presenting a comparative analysis across all time points. Statistical significance between groups was assessed using one-way ANOVA ($p < 0.05$).

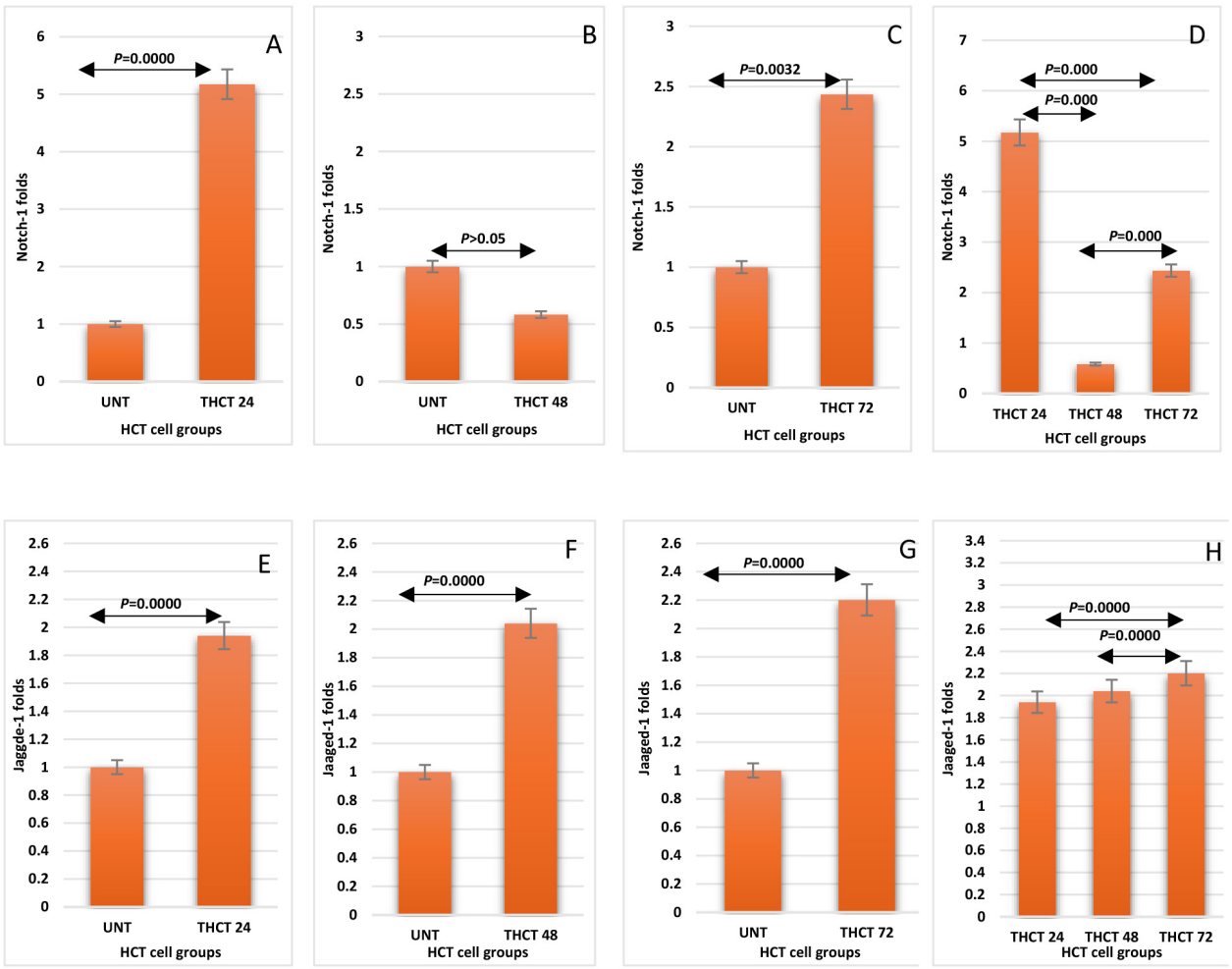

Fig. 4. Temporal changes in *Notch-1* and *Jagged-1* gene expression in HCT cells following carrageenan/soy protein mixture treatment. UNT denotes untreated control cells, while THCT refers to cells treated with the carrageenan/soy protein mixture. Panels illustrate (A) Notch-1 expression at 24 h, (B) Notch-1 at 48 h, (C) Notch-1 at 72 h, and (D) comparative Notch-1 expression across all time intervals. Panels (E–G) present Jagged-1 expression at 24 h, 48 h, and 72 h, respectively, while Panel (H) shows a comparison of Jagged-1 expression across all time intervals. Statistical differences between groups were analyzed using one-way ANOVA ($p < 0.05$).

The expression level of the *Jagged-1* gene in HCT-116 cells exposed to carrageenan/soy protein treatment increased significantly and gradually at 24, 48, and 72 hours compared to 0 hours ($p < 0.001$ for each period) (Fig. 4E–G). Although there was no significant increase in *Jagged-1* mRNA level at 24 hours compared to its level at 48 hours, its expression decreased significantly compared to its level at 72 hours ($p < 0.001$). Furthermore, *Jagged-1* mRNA expression declined significantly at 48 hours compared to 72 hours ($p < 0.001$) (Fig. 4H).

When treated with carrageenan/soy protein, HCT-116 cells showed significant changes in gene activity. *Notch-2* levels jumped significantly at 24 and 72 hours compared to untreated cells ($p < 0.001$ and $p = 0.0005$), with the highest peak at 24 hours (Fig. 5A,C). We also exhibited a notable increase at 48 hours compared to the untreated control (Fig. 5B), although it wasn't statistically significant. For *Notch-2*, we observed its strongest response at 24 hours, much higher than at 48 or 72 hours ($p < 0.001$ for each comparison). Interestingly, *Notch-2* levels dropped significantly at 48 hours before rising again to 72 hours ($p = 0.0107$) (Fig. 5D).

Carrageenan/soy protein dramatically reshaped gene expression in HCT-116 cells. HSE-1 activity surged significantly at 24 hours ($p < 0.001$ versus control), creating a peak response that far outpaced later timepoints ($p < 0.001$ versus both 48 and 72 hours) (Fig. 5E). This initial genetic surge couldn't sustain itself—HSE-1 levels gradually declined, showing only modest elevation at 48 hours (Fig. 5F) before significantly dropping below normal by 72 hours ($p = 0.044$) (Fig. 5G). Meanwhile, *Notch-2* expression followed a different pattern, decreasing consistently at both 48 and 72 hours without a significant difference between these later timepoints (Fig. 5H).

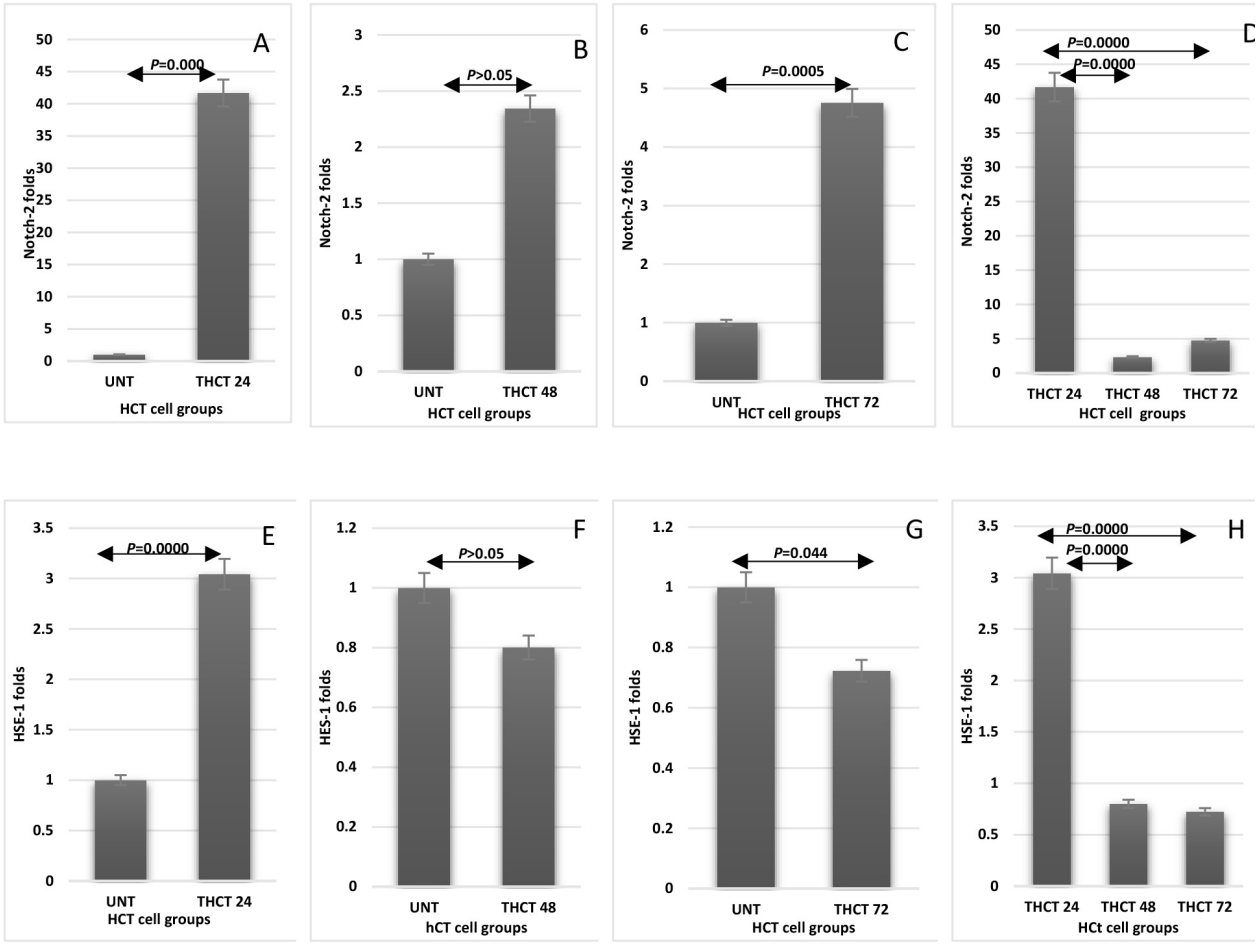

Fig. 5. Temporal changes in *Notch-2* and HSE-1 gene expression in HCT cells following carrageenan/soy protein mixture treatment. Gene expression analysis at sequential timepoints: (A) Notch-2 levels at 24 hours; (B) Notch-2 levels at 48 hours; (C) Notch-2 levels at 72 hours; (D) Notch-2 expression comparison across all time intervals; (E) HSE-1 levels at 24 hours; (F) HSE-1 levels at 48 hours; (G) HSE-1 levels at 72 hours; and (H) HSE-1 expression comparison across all time intervals. Statistical significance between groups was determined using one-way ANOVA ($p < 0.05$). UNT represents untreated control cells, while THCT indicates cells treated with the carrageenan/soy protein mixture.

3.5 Gene Expressions Correlations After an Experiment Over Time

The targeted gene expression analysis of carrageenan/soy protein-treated HCT cells after 24 hours revealed distinct correlation patterns. *BAX* exhibited significant positive relationships with both *Bcl-2* (r = 0.71) and *NF-kB* (r = 0.76), while *Notch-1* and *Notch-2* demonstrated a significant positive correlation (r = 0.91). JAG-1 showed a negative correlation with *Notch-2* (r = –0.52) but positively correlated with *NF-kB* (r = 0.81). *HSE-1* displayed a strong positive alignment with *Bcl-2* (r = 0.849) alongside a significant negative relationship with *Notch-2* (r = –0.75) (Fig. 6).

Otherwise, HCT cells treated with carrageenan/soy protein for 48 hours revealed substantially altered relationship patterns compared to the 24-hour timepoint. After 48 hours, *BAX* showed weak positive correlations with *Bcl-2* (r = 0.16, $p > 0.05$) and *NF-kB* (r = 0.15, $p > 0.05$), contrasting with their previously strong associations. Also, *NF-kB* exhibited a strong negative correlation with *Bcl-2* (r = –0.92, $p < 0.001$) while developing strong positive relationships with Notch 1 (r = 0.90, $p < 0.001$) and *HSE-1* (r = 0.90, $p < 0.001$). Particularly noteworthy was the robust correlation between *HSE-1* and Notch 1 (r = 0.97, $p < 0.0001$), while *Notch-2* showed only moderate correlations with other genes. JAG-1 maintained moderate positive correlations with several genes, including *HSE-1* (r = 0.70, $p < 0.01$) and Notch 1 (r = 0.69, $p < 0.01$) (Fig. 6).

After 72 hours, *BAX* maintained a moderate positive correlation with *Bcl-2* (r = 0.41, $p < 0.05$) and weaker associations with other genes. Notably, *Bcl-2* and Notch 1 displayed a powerful positive correlation (r = 0.95, $p < 0.001$), suggesting synchronized regulation at this time point. *NF-kB* showed a strong positive correlation with *Notch-2* (r =

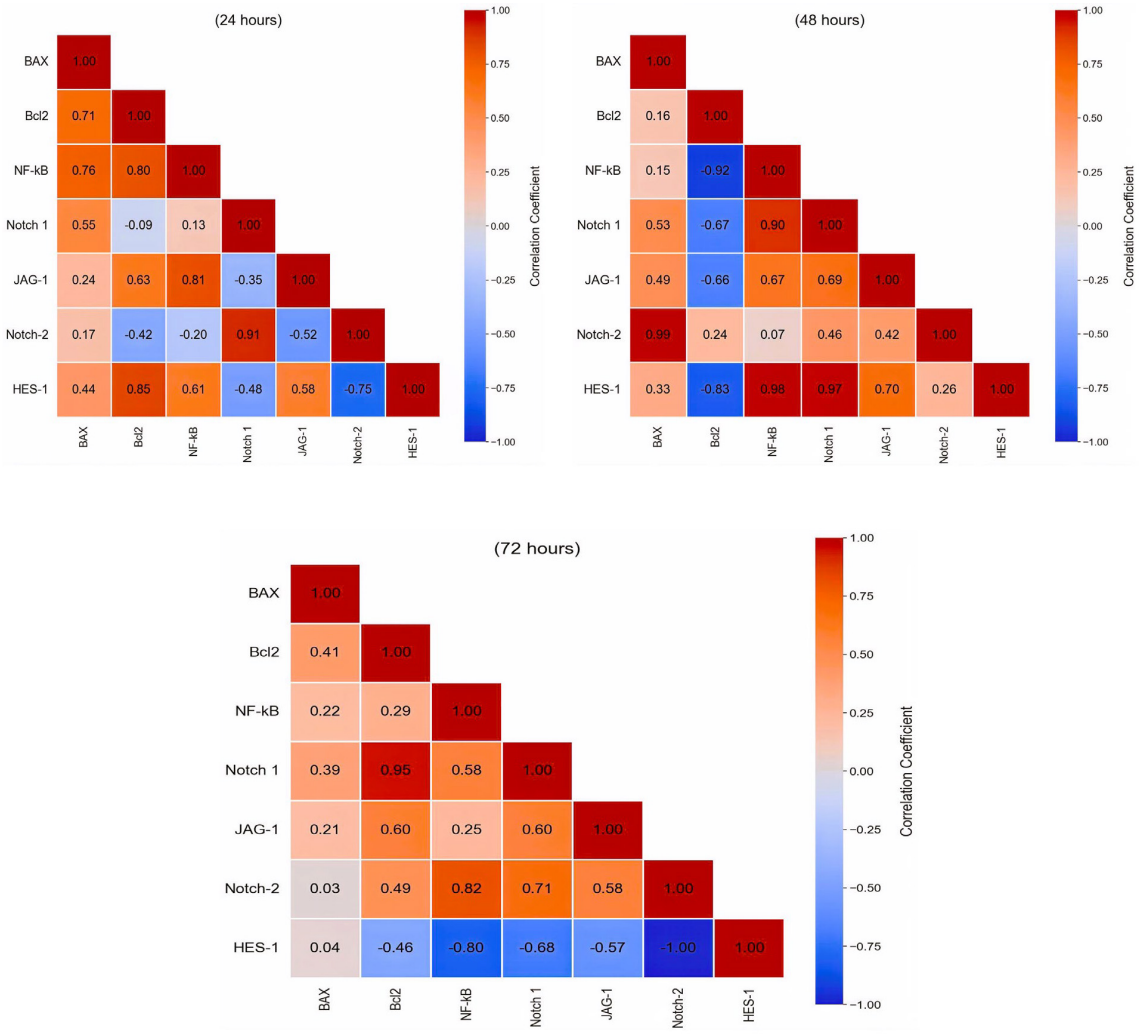

Fig. 6. Illustrates the dynamic changes in genetic interactions within HCT cancer cells following treatment with the carrageenan and soy protein combination. Distinct, color-coded matrices display the gene correlations evolving at 24, 48, and 72 hours. Strong positive associations between genes are marked in vivid red, while strong negative correlations appear as deep blue. The targeted gene correlation analysis was conducted using a robust Python workflow that utilized NumPy for computations, pandas for data management, and seaborn for generating clear and informative heatmaps.

0.82, $p < 0.001$) while developing a strong negative relationship with *HSE-1* (r = –0.80, $p < 0.001$). *HSE-1* exhibited significant negative correlations with nearly all genes, most prominently with *Notch-2* (r = –1.00, $p < 0.0001$) and Notch 1 (r = –0.68, $p < 0.01$). JAG-1 maintained moderate positive correlations with *Bcl-2* (r = 0.60, $p < 0.01$) and Notch 1 (r = 0.60, $p < 0.01$) (Fig. 6).

4. Discussion

The current study confirmed the remarkable efficacy of the carrageenan and soy protein mixture against HCT cells through an intricate temporal progression of cellular transformations and death mechanisms. The current findings illustrate three distinct phases connecting morphological alterations, viability patterns, and molecular signaling networks.

During the initial phase, the mixture rapidly disrupted epithelial integrity within 24 hours. While control cells maintained their characteristic spheroid morphology, with distinct nuclei and microvillous projections, treated cells underwent dramatic remodeling, featuring cytoplasmic retraction and membrane evaginations—classic hallmarks of programmed cell death [34]. This current morphological transformation aligned perfectly with our death marker analysis, showing simultaneous activation of early apoptosis, late apoptosis, and significant necrosis, confirming all the hallmarks of apoptotic progression [35]. The gene expression profile at 24 hours featured a remarkably synchronized response pattern. The current pro-apoptotic *BAX* [36] showed strong positive associations with both anti-apoptotic *BCL-2* [37] and inflammatory mediator *NF-kB* [38], indicating a balanced cellular response [39]. Cur-

rently, *Notch-1* and *Notch-2* demonstrated perfect synchronization while HSE-1 maintained an unexpected positive correlation with *BCL-2*, yet a negative association with *Notch-2*, suggesting activation of non-canonical signaling mechanisms [40]. These current complex interactions triggered comprehensive early activation of Notch components, HSE-1, *NF-kB*, *BAX*, and *BCL-2*, representing a holistic stress-adaptation program simultaneously promoting both survival and death mechanisms [37,41,42].

In the present study, after 48 hours of exposure, a strategic shift emerged in cellular response. Morphologically, cells displayed intensified apoptotic features with pronounced cytosolic compaction and extensive membrane vesiculation [43]. Paradoxically, the current progression coincided with the complete disappearance of early apoptosis markers and a temporary decrease in necrosis, suggesting a transitional phase where cells initially committed to apoptosis were completing their death process. At the same time, necrotic pathways temporarily abated [35]. The current transition phase featured a profound reconfiguration of signaling networks. The strong correlations between current *BAX* and both *BCL-2*/*NF-kB* (observed at 24 h) significantly diminished. *NF-kB* formed a strong inverse relationship with *BCL-2* while establishing positive connections with *Notch-1* and HSE-1, indicating inflammatory signaling had assumed a dominant regulatory role, potentially suppressing conventional anti-apoptotic mechanisms while enhancing alternative survival pathways [39]. The current *BCL-2* stabilized to baseline levels while *NF-kB* moderated but remained elevated, corresponding with the shift from controlled to disorganized cell death [44]. The current viability data supported this interpretation, showing modest recovery from 78.8% to 82.95%, indicating some cellular subpopulations had activated survival mechanisms against the treatment.

In this study, most revealing patterns emerged at hour 72, where three distinct phenomena converged: morphologically, cells reached a "homeostatic plateau" with no further structural changes; viability continued improving to 86.86%; yet paradoxically, necrosis surged dramatically to levels significantly exceeding earlier timepoints. Despite some current HCT cells displaying stabilized architecture and increased flexibility, the carrageenan/soy protein mixture fundamentally compromised essential internal cellular systems, ultimately triggering widespread necrotic collapse. In the present study, further gene expression analysis at 72 hours featured a dramatic shift in signaling relationships. The current *BAX* reached maximum expression while the *BCL-2* plummeted to minimal levels, creating an overwhelmingly pro-death environment [45]. Also, the *NF-kB* activity fell below the untreated control levels precisely when *BAX* peaked and *BCL-2* collapsed, indicating inflammatory pathway withdrawal may have functioned as a molecular trigger for terminal necrosis [46]. Furthermore, the current HSE-1 declined from peak levels to below baseline (untreated control level), concurrent with *BCL-2* suppression and necrosis amplification, suggesting stress protection failure ultimately enabled the massive terminal necrotic surge [47].

The Notch signaling (cell survival genes) [48] analysis verified additional insights into the current mixture response. The current *Notch-1* expression exhibited a wave-like pattern with peaks at 24 and 72 hours separated by a 48-hour depression, closely tracking the oscillating necrotic response. These current findings contrast with *Jagged-1*'s steady increase throughout the experiment. By 72 hours, treated HCT cells established a new equilibrium state where the reestablished moderate *BAX*/*BCL-2* correlation suggested successful navigation through earlier stress phases in surviving cells [37]. The current noticeable *BCL-2*/*Notch-1* relationship indicates that cancer cells repurposed Notch signaling to reinforce their survival mechanisms [49]. Most remarkably, current HSE-1 expression transformed into a master negative regulator, showing inverse correlations with nearly all targeted genes, indicating it functioned as a critical regulatory "brake" stabilizing cellular responses during prolonged exposure [50].

Our findings verified that carrageenan/soy protein mixture acted as a sophisticated therapeutic mechanism, evolving across multiple phases: initial multimodal assault (24 h), adaptive transition (48 h), and terminal necrotic resolution (72 h). This sequence offered significant advantages over conventional cancer treatments that typically engaged single death pathways, which cancer cells often evolved to resist [51]. This biphasic viability response suggested the mixture created a selective pressure that eliminated vulnerable cells while temporarily allowing stress-adapted populations to persist before eventual necrotic elimination [52]. The dramatic rise in necrosis at 72 hours, despite morphological stabilization, suggested that carrageenan/soy protein targeted metabolic and bioenergetic systems that remained functional long enough to maintain cellular architecture but ultimately collapsed [53]. This mechanism could prove especially valuable against therapy-resistant cancer cells that have evolved robust anti-apoptotic defenses but remain vulnerable to metabolic disruption [13]. These molecular dynamics suggested promising therapeutic opportunities: combining carrageenan/soy protein with *BCL-2* or γ-secretase inhibitors during early response could enhance initial apoptotic death. In contrast, HSE-1 inhibitors at 48 hours might prevent stress adaptation and accelerate the elimination of resistant cell populations. Additionally, the complete absence of early apoptosis after 24 hours indicated that treatment timing was critical, suggesting pulsed administration protocols might optimize therapeutic efficacy by repeatedly reinitiating the early apoptotic response while maintaining necrotic pressure [54].

5. Conclusion

Our findings demonstrate that the carrageenan–soy protein mixture induces a distinct and multifaceted death response in colon cancer cells, clearly diverging from the mechanisms targeted by conventional therapeutic strategies. Rather than relying on a single apoptosis pathway that is frequently bypassed by resistant cancer phenotypes, this mixture orchestrated a sequential cascade: an early multimodal cytotoxic assault at 24 hours, followed by an adaptive transition phase at 48 hours, and culminating in a necrotic collapse by 72 hours. The paradox observed at the 72-hour time point—where transient improvements in cellular morphology and viability metrics coincided with catastrophic necrotic failure—highlights the potential of this mixture to compromise core metabolic and bioenergetic systems while temporarily preserving structural integrity.

Importantly, the associated reconfiguration of apoptotic gene expression, particularly the emergence of HSE-1 as a master negative regulator, uncovers novel molecular control points that merit deeper exploration. From a translational perspective, these insights suggest that carrageenan–soy protein formulations may provide a basis for developing innovative therapeutic strategies with the capacity to overcome apoptotic resistance in aggressive colorectal cancers. As such, this approach holds promising clinical application value, warranting further *in vivo* validation and preclinical evaluation to establish its safety, efficacy, and potential integration into future colorectal cancer treatment regimens.

Significant Statement

This groundbreaking study revealed that carrageenan-soy protein mixture induced a unique triphasic death response in colon cancer cells, orchestrating a remarkable 72-hour paradox where improved cellular appearance masked catastrophic metabolic collapse—a potentially revolutionary approach for defeating therapy-resistant cancers by exploiting temporal gene regulatory reprogramming rather than targeting single death pathways.

Availability of Data and Materials

The data that support the findings of this study are available within this published article. The datasets used and analyzed during the current study are available from the corresponding author upon reasonable request.

Author Contributions

AA and SA conceived the study. SA designed and conducted experiments, including all animal procedures and data analysis. AA wrote and reviewed the manuscript. Both authors contributed to editorial changes in the manuscript. Both authors read and approved the final manuscript. Both authors have participated sufficiently in the work and agreed to be accountable for all aspects of the work.

Ethics Approval and Consent to Participate

Not applicable.

Acknowledgment

We would like to express our gratitude to all those who helped me during the writing of this manuscript.

Funding

This research received no external funding.

Conflict of Interest

The authors declare no conflict of interest.

References

[1] Sun Y, Keat OB, Rajabi S. The role of physical activity and epigenetic changes in colorectal cancer prevention. Cancer Cell International. 2025; 25: 227. https://doi.org/10.1186/s12935-025-03872-1.

[2] Dakal TC, Dhabhai B, Pant A, Moar K, Chaudhary K, Yadav V, *et al*. Oncogenes and tumor suppressor genes: functions and roles in cancers. MedComm. 2024; 5: e582. https://doi.org/10.1002/mco2.582.

[3] Basak D, Arrighi S, Darwiche Y, Deb S. Comparison of Anticancer Drug Toxicities: Paradigm Shift in Adverse Effect Profile. Life (Basel, Switzerland). 2021; 12: 48. https://doi.org/10.3390/life12010048.

[4] Yan L, Shi J, Zhu J. Cellular and molecular events in colorectal cancer: biological mechanisms, cell death pathways, drug resistance and signalling network interactions. Discover Oncology. 2024; 15: 294. https://doi.org/10.1007/s12672-024-01163-1.

[5] Nishida A, Andoh A. The Role of Inflammation in Cancer: Mechanisms of Tumor Initiation, Progression, and Metastasis. Cells. 2025; 14: 488. https://doi.org/10.3390/cells14070488.

[6] Glaviano A, Foo ASC, Lam HY, Yap KCH, Jacot W, Jones RH, *et al*. PI3K/AKT/mTOR signaling transduction pathway and targeted therapies in cancer. Molecular Cancer. 2023; 22: 138. https://doi.org/10.1186/s12943-023-01827-6.

[7] Amodio V, Vitiello PP, Bardelli A, Germano G. DNA repair-dependent immunogenic liabilities in colorectal cancer: opportunities from errors. British Journal of Cancer. 2024; 131: 1576–1590. https://doi.org/10.1038/s41416-024-02848-8.

[8] Li Q, Geng S, Luo H, Wang W, Mo YQ, Luo Q, *et al*. Signaling pathways involved in colorectal cancer: pathogenesis and targeted therapy. Signal Transduction and Targeted Therapy. 2024; 9: 266. https://doi.org/10.1038/s41392-024-01953-7.

[9] Zafar A, Khatoon S, Khan MJ, Abu J, Naeem A. Advancements and limitations in traditional anti-cancer therapies: a comprehensive review of surgery, chemotherapy, radiation therapy, and hormonal therapy. Discover Oncology. 2025; 16: 607. https://doi.org/10.1007/s12672-025-02198-8.

[10] Liu H-Y, Jay M, Chen X. The Role of Nature-Based Solutions for Improving Environmental Quality, Health and Well-Being. Sustainability. 2021; 13: 10950. https://doi.org/10.3390/su131910950.

[11] Liu Z, Gao T, Yang Y, Meng F, Zhan F, Jiang Q, *et al*. Anti-Cancer Activity of Porphyran and Carrageenan from Red Seaweeds. Molecules (Basel, Switzerland). 2019; 24: 4286. https://doi.org/10.3390/molecules24234286.

[12] Fan Y, Wang M, Li Z, Jiang H, Shi J, Shi X, *et al*. Intake of Soy, Soy Isoflavones and Soy Protein and Risk of Cancer Incidence and Mortality. Frontiers in Nutrition. 2022; 9: 847421. https://doi.org/10.3389/fnut.2022.847421.

[13] Hadad SE, Alzahrani S, Alhebshi A, Alrahimi J. Impact of Carrageenan-Soy Protein Combination on CXCR-4 Expression, Cell Viability, and Apoptosis in HCT-116 Cells. Archives of Pharmacy Practice. 2024; 15: 53–62. https://doi.org/10.51847/CZ6T8kG5lr.

[14] Orlandi G, Roncucci L, Carnevale G, Sena P. Different Roles of Apoptosis and Autophagy in the Development of Human Colorectal Cancer. International Journal of Molecular Sciences. 2023; 24: 10201. https://doi.org/10.3390/ijms241210201.

[15] Vujović T, Paradžik T, Babić Brčić S, Piva R. Unlocking the Therapeutic Potential of Algae-Derived Compounds in Hematological Malignancies. Cancers. 2025; 17: 318. https://doi.org/10.3390/cancers17020318.

[16] Wei Q, Zhang YH. Flavonoids with Anti-Angiogenesis Function in Cancer. Molecules. 2024; 29: 1570. https://doi.org/10.3390/molecules29071570.

[17] Wang Z, Yang Z, Qu C, Li J, Wang X. Natural killer cells strengthen antitumor activity of cisplatin by immunomodulation and ameliorate cisplatin-induced side effects. International Urology and Nephrology. 2023; 55: 1957–1970. https://doi.org/10.1007/s11255-023-03650-w.

[18] Garg P, Malhotra J, Kulkarni P, Horne D, Salgia R, Singhal SS. Emerging Therapeutic Strategies to Overcome Drug Resistance in Cancer Cells. Cancers. 2024; 16: 2478. https://doi.org/10.3390/cancers16132478.

[19] Nascimento-Gonçalves E, Mendes BAL, Silva-Reis R, Faustino-Rocha AI, Gama A, Oliveira PA. Animal Models of Colorectal Cancer: From Spontaneous to Genetically Engineered Models and Their Applications. Veterinary Sciences. 2021; 8: 59. https://doi.org/10.3390/vetsci8040059.

[20] Nurkolis F, Taslim NA, Lee D, Park MN, Moon S, Hardinsyah H, *et al*. Mechanism of Action of Isoflavone Derived from Soy-Based Tempeh as an Antioxidant and Breast Cancer Inhibitor via Potential Upregulation of miR-7-5p: A Multimodal Analysis Integrating Pharmacoinformatics and Cellular Studies. Antioxidants. 2024; 13: 632. https://doi.org/10.3390/antiox13060632.

[21] Naponelli V, Piscazzi A, Mangieri D. Cellular and Molecular Mechanisms Modulated by Genistein in Cancer. International Journal of Molecular Sciences. 2025; 26: 1114. https://doi.org/10.3390/ijms26031114.

[22] Pejčić T, Zeković M, Bumbaširević U, Kalaba M, Vovk I, Bensa M, *et al*. The Role of Isoflavones in the Prevention of Breast Cancer and Prostate Cancer. Antioxidants. 2023; 12: 368. https://doi.org/10.3390/antiox12020368.

[23] Lee YJ, Lee C, Choi D, Lee Y, Lee SH. Effect of Soy Isoflavone on Prostate Cancer Cell Apoptosis Through Inhibition of STAT3, ERK, and AKT. Current Issues in Molecular Biology. 2024; 46: 12512–12526. https://doi.org/10.3390/cimb46110743.

[24] Varinska L, Gal P, Mojzisova G, Mirossay L, Mojzis J. Soy and breast cancer: focus on angiogenesis. International Journal of Molecular Sciences. 2015; 16: 11728–11749. https://doi.org/10.3390/ijms160511728.

[25] Wójciak M, Drozdowski P, Skalska-Kamińska A, Zagórska-Dziok M, Ziemlewska A, Nizioł-Łukaszewska Z, *et al*. Protective, Anti-Inflammatory, and Anti-Aging Effects of Soy Isoflavones on Skin Cells: An Overview of In Vitro and In Vivo Studies. Molecules. 2024; 29: 5790. https://doi.org/10.3390/molecules29235790.

[26] Goh YX, Jalil J, Lam KW, Husain K, Premakumar CM. Genistein: A Review on its Anti-Inflammatory Properties. Frontiers in Pharmacology. 2022; 13: 820969. https://doi.org/10.3389/fphar.2022.820969.

[27] Ghadiri N, Javidan M, Sheikhi S, Taştan Ö, Parodi A, Liao Z, *et al*. Bioactive peptides: an alternative therapeutic approach for cancer management. Frontiers in Immunology. 2024; 15: 1310443. https://doi.org/10.3389/fimmu.2024.1310443.

[28] Silva OLT, Alves MGDCF, Rocha HAO. Exploring the Pharmacological Potential of Carrageenan Disaccharides as Antitumor Agents: An In Silico Approach. Marine Drugs. 2024; 23: 6. https://doi.org/10.3390/md23010006.

[29] Kimilu N, Gładyś-Cieszyńska K, Pieszko M, Mańkowska-Wierzbicka D, Folwarski M. Carrageenan in the Diet: Friend or Foe for Inflammatory Bowel Disease? Nutrients. 2024; 16: 1780. https://doi.org/10.3390/nu16111780.

[30] Jabeen F, Zil-E-Aimen, Ahmad R, Mir S, Awwad NS, Ibrahium HA. Carrageenan: structure, properties and applications with special emphasis on food science. RSC Advances. 2025; 15: 22035–22062. https://doi.org/10.1039/d5ra03296b.

[31] Xiang Z, Ma B, Pei X, Wang W, Gong W. Mechanism of action of genistein on breast cancer and differential effects of different age stages. Pharmaceutical Biology. 2025; 63: 141–155. https://doi.org/10.1080/13880209.2025.2469607.

[32] Ağagündüz D, Cocozza E, Cemali Ö, Bayazıt AD, Nanì MF, Cerqua I, *et al*. Understanding the role of the gut microbiome in gastrointestinal cancer: A review. Frontiers in Pharmacology. 2023; 14: 1130562. https://doi.org/10.3389/fphar.2023.1130562.

[33] Rahman U, Younas Z, Ahmad I, Yousaf T, Latif R, Rubab U, *et al*. Enhancing health and therapeutic potential: innovations in the medicinal and pharmaceutical properties of soy bioactive compounds. Frontiers in Pharmacology. 2024; 15: 1397872. https://doi.org/10.3389/fphar.2024.1397872.

[34] Syed Abdul Rahman SN, Abdul Wahab N, Abd Malek SN. In Vitro Morphological Assessment of Apoptosis Induced by Antiproliferative Constituents from the Rhizomes of Curcuma zedoaria. Evidence-based Complementary and Alternative Medicine. 2013; 2013: 257108. https://doi.org/10.1155/2013/257108.

[35] Mustafa M, Ahmad R, Tantry IQ, Ahmad W, Siddiqui S, Alam M, *et al*. Apoptosis: A Comprehensive Overview of Signaling Pathways, Morphological Changes, and Physiological Significance and Therapeutic Implications. Cells. 2024; 13: 1838. https://doi.org/10.3390/cells13221838.

[36] Wolf P, Schoeniger A, Edlich F. Pro-apoptotic complexes of BAX and BAK on the outer mitochondrial membrane. Biochimica et Biophysica Acta. Molecular Cell Research. 2022; 1869: 119317. https://doi.org/10.1016/j.bbamcr.2022.119317.

[37] Qian S, Wei Z, Yang W, Huang J, Yang Y, Wang J. The role of BCL-2 family proteins in regulating apoptosis and cancer therapy. Frontiers in Oncology. 2022; 12: 985363. https://doi.org/10.3389/fonc.2022.985363.

[38] Barnabei L, Laplantine E, Mbongo W, Rieux-Laucat F, Weil R. NF-κB: At the Borders of Autoimmunity and Inflammation. Frontiers in Immunology. 2021; 12: 716469. https://doi.org/10.3389/fimmu.2021.716469.

[39] Moawadh MS, Mir R, Tayeb FJ, Asim O, Ullah MF. Molecular Evaluation of the Impact of Polymorphic Variants in Apoptotic (Bcl-2/Bax) and Proinflammatory Cytokine (TNF-α/IL-8) Genes on the Susceptibility and Progression of Myeloproliferative Neoplasms: A Case-Control Biomarker Study. Current Issues in Molecular Biology. 2023; 45: 3933–3952. https://doi.org/10.3390/cimb45050251.

[40] Jo YW, Park I, Yoo K, Woo HY, Kim YL, Kim YE, *et al*. Notch1 and Notch2 Signaling Exclusively but Cooperatively Maintain Fetal Myogenic Progenitors. Stem Cells. 2022; 40: 1031–1042. https://doi.org/10.1093/stmcls/sxac056.

[41] Hussar P. Apoptosis Regulators Bcl-2 and Caspase-3. Encyclopedia. 2022; 2: 1624–1636. https://doi.org/10.3390/encyclopedia2040111.

[42] Perez-Serna AA, Guzman-Llorens D, Dos Santos RS, Marroqui L. Bcl-2 and Bcl-xL in Diabetes: Contributions to Endocrine Pancreas Viability and Function. Biomedicines. 2025; 13: 223.

https://doi.org/10.3390/biomedicines13010223.
[43] Jeppesen DK, Zhang Q, Franklin JL, Coffey RJ. Extracellular vesicles and nanoparticles: emerging complexities. Trends in Cell Biology. 2023; 33: 667–681. https://doi.org/10.1016/j.tcb.2023.01.002.
[44] Palabiyik AA. The role of Bcl 2 in controlling the transition between autophagy and apoptosis (Review). Molecular Medicine Reports. 2025; 32: 172. https://doi.org/10.3892/mmr.2025.13537.
[45] Barillé-Nion S, Lohard S, Juin PP. Targeting of BCL-2 Family Members during Anticancer Treatment: A Necessary Compromise between Individual Cell and Ecosystemic Responses? Biomolecules. 2020; 10: 1109. https://doi.org/10.3390/biom10081109.
[46] Rizq AT, Sirwi A, El-Agamy DS, Abdallah HM, Ibrahim SRM, Mohamed GA. Cepabiflas B and C as Novel Anti-Inflammatory and Anti-Apoptotic Agents against Endotoxin-Induced Acute Kidney and Hepatic Injury in Mice: Impact on Bax/Bcl2 and Nrf2/NF-κB Signalling Pathways. Biology. 2023; 12: 938. https://doi.org/10.3390/biology12070938.
[47] Vázquez-Galán YI, Guzmán-Silahua S, Trujillo-Rangel WÁ, Rodríguez-Lara SQ. Role of Ischemia/Reperfusion and Oxidative Stress in Shock State. Cells. 2025; 14: 808. https://doi.org/10.3390/cells14110808.
[48] Zhou B, Lin W, Long Y, Yang Y, Zhang H, Wu K, *et al*. Notch signaling pathway: architecture, disease, and therapeutics. Signal Transduction and Targeted Therapy. 2022; 7: 95. https://doi.org/10.1038/s41392-022-00934-y.
[49] Vogler M, Braun Y, Smith VM, Westhoff MA, Pereira RS, Pieper NM, *et al*. The BCL2 family: from apoptosis mechanisms to new advances in targeted therapy. Signal Transduction and Targeted Therapy. 2025; 10: 91. https://doi.org/10.1038/s41392-025-02176-0.
[50] Sabatier P, Beusch CM, Saei AA, Aoun M, Moruzzi N, Coelho A, *et al*. An integrative proteomics method identifies a regulator of translation during stem cell maintenance and differentiation. Nature Communications. 2021; 12: 6558. https://doi.org/10.1038/s41467-021-26879-4.
[51] Lei ZN, Tian Q, Teng QX, Wurpel JND, Zeng L, Pan Y, *et al*. Understanding and targeting resistance mechanisms in cancer. MedComm. 2023; 4: e265. https://doi.org/10.1002/mco2.265.
[52] Bollen C, Louwagie E, Verstraeten N, Michiels J, Ruelens P. Environmental, mechanistic and evolutionary landscape of antibiotic persistence. EMBO Reports. 2023; 24: e57309. https://doi.org/10.15252/embr.202357309.
[53] Qiao D, Zhang Y, Sun F, Yoo M, Zhao G, Zhang B. Enhancement mechanism of ι-carrageenan on the network structure and gel-related properties of soy protein isolate/λ-carrageenan system. Food Chemistry. 2025; 468: 142476. https://doi.org/10.1016/j.foodchem.2024.142476.
[54] Iuliano L, Dalla E, Picco R, Mallavarapu S, Minisini M, Malavasi E, *et al*. Proteotoxic stress-induced apoptosis in cancer cells: understanding the susceptibility and enhancing the potency. Cell Death Discovery. 2022; 8: 407. https://doi.org/10.1038/s41420-022-01202-2.